COMPDYN 2025
10th ECCOMAS Thematic Conference on
Computational Methods in Structural Dynamics and Earthquake Engineering
M. Papadrakakis, M. Fragiadakis (eds.)
Rhodes Island, Greece, 15-18 June 2025

EXPERIMENTAL CONTROL OF THE MECHANICAL PROPERTIES OF PRESSURIZED FLUID VISCOUS DAMPERS OVER TWENTY YEARS AFTER THEIR PRODUCTION

Gloria Terenzi[1], Stefano Sorace[2], Carlo Vienni[3]

[1,3] Department of Civil and Environmental Engineering, University of Florence, Italy
Via S. Marta 3, 50139 Florence, Italy
e-mail: gloria.terenzi@unifi.it, carlo.vienni@unifi.it

[2] Polytechnic Department of Engineering and Architecture, University of Udine, Udine, Italy
Via delle Scienze 206, 33100 Udine, Italy
stefano.sorace@uniud.it

Abstract

The stability over time of the mechanical properties of seismic dampers is a fundamental requirement to guarantee the maintenance of their protective action on the buildings and infrastructures where they are installed. This requirement can only be checked experimentally, by repeating at a considerable interval of time the qualification tests carried out on the devices immediately after their production. This topic is addressed in the paper, focusing on Pressurized Fluid Viscous (PFV) dampers, which have been the subject of over than twenty-five years of research activities by the first two authors. During the first season of these activities, several testing campaigns have been developed on various types of PFV devices, which allowed identifying their mechanical characteristics. Some of the experimental investigations carried out in the early 2000s are currently being repeated on the same devices tested at that time. A synthesis of the new laboratory campaign completed on a first pair of PFV spring-damper is presented herein, comparing the results with those of the original qualification tests. The identification process developed on both data sets allows to assess a complete stability of the mechanical properties and response capacities of the examined devices over this significantly long-time span.

Keywords: Supplemental damping devices, Pressurized fluid viscous dampers, Experimental tests, Mechanical characterization, Aging effects.

1 INTRODUCTION

Periodic on-site inspections are normatively imposed for the visual control of the maintenance conditions of dampers incorporated in seismic protection systems of structures and infrastructures. Due to the considerable technical problems and associated costs, experimental verification activities—either developed on-site or by temporarily uninstalling and testing the devices in laboratory—are performed only in special cases. This does not allow to adequately investigate possible time-delayed effects on the mechanical properties and response capacities of devices, several years or even decades after their original test qualification and installation. Furthermore, very few experimental research studies on this topic are reported in the literature.

This is also the case of pressurized fluid viscous (PFV) dissipaters, whose application dates back to the end of the 19th century in railway engineering, and to the 1980s in structural earthquake engineering [1]. In view of this, a study has recently been undertaken by the authors, aimed at duplicating the quasi-static and dynamic characterization campaigns carried out on elements originally tested in research and design activities from 2001 to 2008 [2-3], so as to assess possible changes in their hysteretic properties about twenty years after their production.

The results of the tests recently completed on a first pair of commercial PFV spring-damper, as well as of relevant identification analyses, are summarized in this paper. Comparisons between the original and the current cyclic response of the devices under several different strain rates show almost coincident outputs, and thus a substantial stability of the damping and stiffness characteristics over time.

2 MECHANICAL CHARACTERISTICS OF PFV SPRING-DAMPERS

The mechanical behaviour of the considered class of fluid viscous devices, whose working principle is based on the flow of a pressurized highly viscous fluid through a thin annular space between piston head and tank casing [2], is characterized by the following damping, F_d, and elastic, F_{ne}, force components:

$$F_d(t) = csgn[\dot{x}(t)]|\dot{x}(t)|^{\gamma} \tag{1}$$

$$F_{ne}(t) = k_2 x(t) + \frac{(k_1 - k_2)x(t)}{\left[1 + \left|\frac{k_1 x(t)}{F_0}\right|^5\right]^{1/5}} \tag{2}$$

where: t = time variable; c = damping coefficient; $sgn(\cdot)$ = signum function; $\dot{x}(t)$ = velocity; $|\cdot|$ absolute value: γ = fractional exponent, ranging from 0.1 to 0.2; F_0 = static pre-load; k_1, k_2 = stiffness of the response branches situated below and beyond F_0; and $x(t)$ = displacement.

The two force components coexist in PFV spring-dampers, which are mostly installed in dissipative bracing systems [3-4], where they are mounted in pairs, with pistons driven in half-stroke position at the tip of the supporting inverted V-shaped steel trusses, so as to achieve a symmetric tension-compression response capacity. In this configuration, by considering that the piston motion starts when the external force is equal to F_0+F_d, and thus when the response occurs along the second branch of the nonlinear elastic law (2), the latter can be simplified by the following linear expression, F_e:

$$F_e(t) = k_2 x(t) \tag{3}$$

According to these relations, named d_{max} the stroke, the cyclic behaviour of a PFV spring-damper with piston in initial half-stroke position is schematized in Figure 1, where $\pm d_{max}/2$ is the resulting available displacement after the installation.

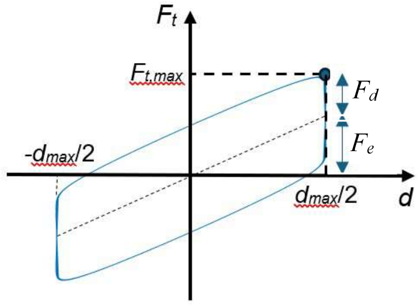

Figure 1: Schematized response cycle of a PFV spring-damper with piston driven in half-stroke initial position.

3 EXPERIMENTAL RESULTS

Figure 2 shows a photographic image of the first PFV spring-dampers tested in the early 2000s and 2025 characterization campaigns, and their assembly in the experimental apparatus set up at the Structural Laboratory of the University of Basilicata, Potenza, Italy. Consistently with the installation layout in real dissipative bracing applications [3-4], the devices are mounted in pair and in half-stroke position. The latter is reached by acting on two threaded steel bars screwed to two orthogonal contrast plates, as highlighted in Figure 2.

The two campaigns were developed by imposing several harmonic displacement time-histories with different frequencies and amplitudes. Among other testing programmes of the early 2000s, the results synthesized below refer to the concluding series, carried out in 2008.

The most significant response data are summarized in Tables 1 and 2, where the tests are numbered from T1 to T12, and the following quantities are listed: ν, d_i = frequency and nominal peak values of the imposed harmonic displacement histories; $d_{exp,max+}$, $d_{exp,max-}$ = experimentally measured maximum positive and negative response displacements; $d_{exp,mean}$ = mean absolute value of response displacements; $v_{exp,max}$ = maximum response velocities; c_{id} = damping coefficient values identified from test results; $E_{D,exp}$ = experimentally measured values of the dissipated energy; $E_{D,comp}$ = computed values of the dissipated energy, evaluated by imposing displacement time-histories with peak positive and negative values equal to $d_{exp,mean}$ and the force histories measured in the tests.

The response cycles obtained in the 2008 and 2025 tests are graphically represented, in superimposition, in Figures 3 through 10.

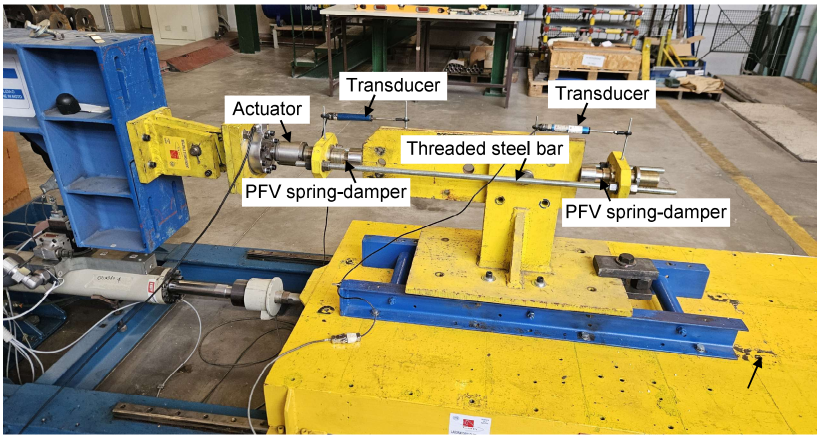

Figure 2: Image of the PFV spring-damper pair tested in the 2008 and 2025 cyclic characterization campaigns, and its assembly in the experimental apparatus.

Test Nr.	ν [Hz]	d_i [mm]	$d_{exp,max+}$ [mm]	$d_{exp,max-}$ [mm]	$d_{exp,mean}$ [mm]	$v_{exp,max}$ [mm/s]	c_{id} kN(s/mm)$^{\gamma}$	$E_{D,exp}$ (kN·mm)	$E_{D,comp}$ (kN·mm)
T1	0.01	5	4.13	-4.13	4.13	0.26	8.53	101.2	101.1
T2	0.01	14	12.44	-12.53	12.49	0.78	8.74	794.9	794.6
T3	0.1	14	11.31	-10.49	10.90	6.8	6.69	2137.8	2139.3
T4	0.5	14	10.74	-9.84	10.29	32.3	6.85	2145.5	2145.7
T5	1.0	14	10.46	-9.62	10.04	63.1	6.76	2627.6	2626.5
T6	2.0	5	2.98	-1.89	2.44	30.6	5.98	287.5	287.7
T11	2.0	10	7.81	-8.36	8.08	101.5	5.70	4080.1	4084
T7	4.0	5	3.73	-2.99	3.36	84.5	5.37	449.8	448.5
T10	4.0	10	8.56	-8.56	8.56	215.2	5.59	4942.9	4952.7
T8	5.0	5	3.69	-2.95	3.32	104.3	5.65	265.8	265.2
T9	5.0	10	7.97	-8.27	8.11	254.4	5.85	3252	3257.6
T12	8.0	10	7.75	-8.69	8.22	412.2	5.85	5889.4	5896.2

Table 1: Measured and computed response data from 2008 tests.

Test Nr.	ν [Hz]	d_i [mm]	$d_{exp,max+}$ [mm]	$d_{exp,max-}$ [mm]	$d_{exp,mean}$ [mm]	$v_{exp,max}$ [mm/s]	c_{id} kN(s/mm)$^{\gamma}$	$E_{D,exp}$ (kN·mm)	$E_{D,comp}$ (kN·mm)
T1	0.01	5	3.98	-3.75	3.87	0.24	8.74	84.8	84.8
T2	0.01	14	11.21	-12.22	11.71	0.74	8.87	746.1	794.1
T3	0.1	14	10.19	-9.88	10.03	6.3	6.76	1957.5	1951.0
T4	0.5	14	9.58	-9.34	9.46	29.7	6.52	2255.1	2255.3
T5	1.0	14	9.86	-9.31	9.58	60.2	6.42	2362.4	2361.5
T6	2.0	5	2.68	-1.83	2.25	28.3	5.58	292.5	292.2
T11	2.0	10	5.75	-6.58	6.16	77.4	5.86	3304	3303.1
T7	4.0	5	2.52	-1.72	2.12	53.3	5.80	483.6	483.3
T10	4.0	10	5.70	-6.13	5.92	148.8	5.82	3716.9	3717.4
T8	5.0	5	2.41	-1.69	2.05	64.4	5.90	155.5	154.9
T9	5.0	10	5.75	-6.73	6.24	195.9	5.92	2396.9	2396.8
T12	8.0	10	5.66	-6.54	6.11	307.1	5.83	3389.8	3388

Table 2: Measured and computed response data from 2025 tests.

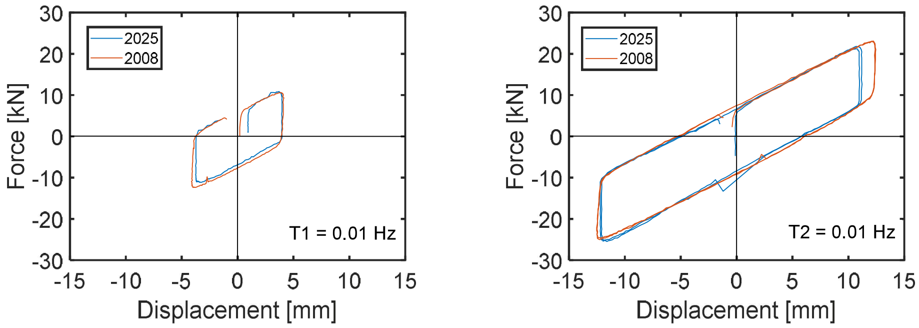

Figure 3: Response cycles obtained from 2008 and 2025 tests T1 and T2, with ν = 0.01 Hz.

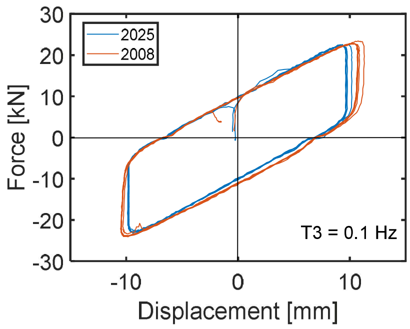

Figure 4: Response cycles obtained from 2008 and 2025 tests T3, with ν = 0.1 Hz.

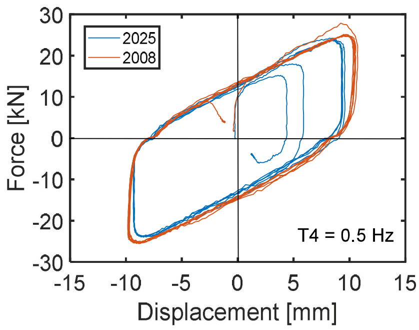

Figure 5: Response cycles obtained from 2008 and 2025 tests T4, with ν = 0.5 Hz.

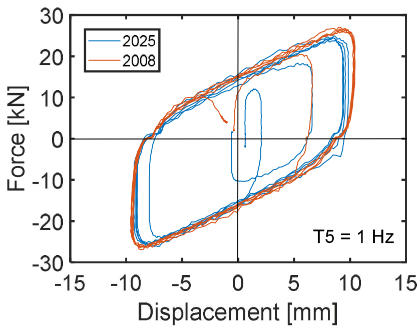

Figure 6: Response cycles obtained from 2008 and 2025 tests T5, with ν = 1 Hz.

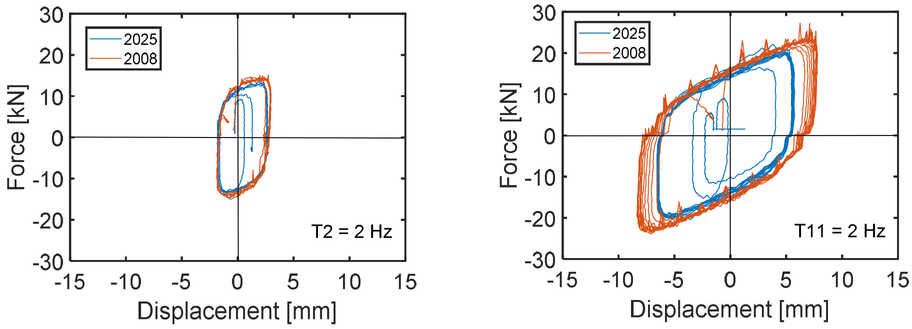

Figure 7: Response cycles obtained from 2008 and 2025 tests T2 and T11, with ν = 2 Hz.

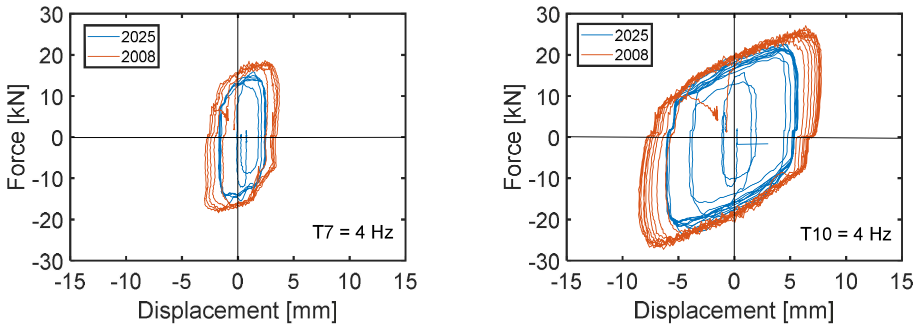

Figure 8: Response cycles obtained from 2008 and 2025 tests T7 and T10, with ν = 4 Hz.

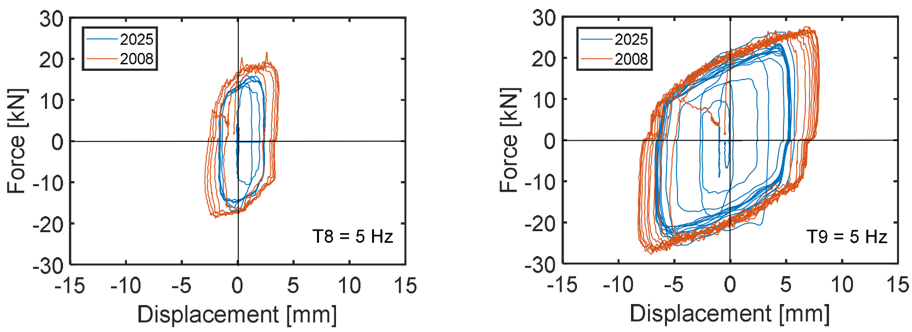

Figure 9: Response cycles obtained from 2008 and 2025 tests T8 and T9, with ν = 5 Hz.

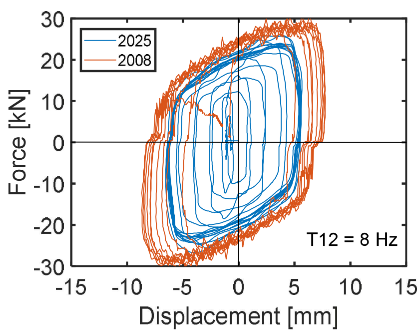

Figure 10: Response cycles obtained from 2008 and 2025 tests T12, with ν = 8 Hz.

By processing the test data, the possible aging effects on the two devices were assessed by comparing the mechanical properties estimated from the response obtained in the past campaign and in the new one.

Concerning the elastic component F_e, an identical k_2 value of 1.4 kN/mm was identified from the two test sets. The velocity exponent γ shows a stable value of 0.2. The c_{id} estimates derived from the identification process are plotted as a function of $v_{exp,max}$ in Figure 11, where blue "o" and red "+" symbols refer to the 2008 and 2025 tests, respectively.

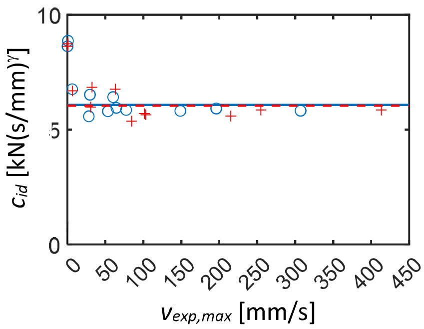

Figure 11: Damping coefficient values identified from the results of the 2008 and 2025 experimental campaigns, as a function of the maximum response velocity.

The first four points of the two series (tests T1-T4) concern the frequencies of 0.01 Hz ($v_{exp,max}$ = 0.62 mm/s), for two d_i values, 0.1 Hz ($v_{exp,max}$ = 6.2 mm/s), and 0.5 Hz ($v_{exp,max}$ = 31 mm/s), which correspond to quasi-static testing conditions. The c_{id} values are very similar for the two series, reaching a maximum of 8.87 kN(s/mm)^γ in the T1 tests. Starting from the T5 tests, carried out at a frequency of 1 Hz, c_{id} appears stable, with mean values of 6.08 kN(s/mm)^γ for the 2008 tests (blue straight line), and 6.04 kN(s/mm)^γ (red dotted line), for the 2025 tests. These nearly coincident mean values highlight that the mechanical behaviour of the first two PFV spring-dampers examined is not affected by any appreciable aging effects.

4 CONCLUSIONS

- The results of the new testing campaign carried out on the first PFV spring-damper pair examined in this study show very similar values of its mechanical characteristics to those derived from the 2008 tests.
- This applies to the second-branch stiffness of the non-linear elastic spring component, k_2, equal to 1.4 kN/mm in both cases.
- At the same time, the identification analysis of the damping coefficient, which in principle could be the most sensitive parameter to the aging effects, highlights almost coincident mean values for the two data sets, both in quasi-static and dynamic response conditions.
- For the latter, values within a narrow range around 6 kN(s/mm)^γ are always obtained, starting from frequencies of 2 Hz up to 8 Hz, corresponding to applied velocities from 103 mm/s to 412 mm/s.
- Although limited to a single pair of devices, the results of this first section of the study support the hypothesis of negligible aging effects on the response capacities of pressurized fluid viscous dampers.

ACKNOWLEDGMENTS

The study reported in this paper was sponsored by the Italian Department of Civil Protection within the ReLUIS-DPC Project 2024/2026, WP 15 "Devices and systems for base isolation and supplemental damping dissipation". The authors gratefully acknowledge this financial support.

REFERENCES

[1] Dyna Shock System. URL http:// www.dynashocksystem.com/.

[2] S. Sorace, G. Terenzi, Non-linear dynamic modelling and design procedure of FV spring-dampers for base isolation. *Engineering Structures*, **23**,1556–1567, 2001.

[3] S. Sorace, G. Terenzi, Seismic protection of frame structures by fluid viscous damped braces. *ASCE Journal of Structural Engineering*, **134**, 45–55, 2008.

[4] S. Sorace, G. Terenzi, F. Fadi, Shaking table and numerical seismic performance evaluation of a fluid viscous-dissipative bracing system. *Earthquake Spectra,* **28**, 1619–1642, 2012.